Silicon-photonic PTAT temperature sensor for micro-ring resonator thermal stabilization

Saman Saeedi* **and Azita Emami**

Department of Electrical Engineering, California Institute of Technology, 1200 E California Blvd, Pasadena, California 91125, USA

ssaeedi@caltech.edu

Abstract: We present a scheme for thermal stabilization of micro-ring resonator modulators through direct measurement of ring temperature using a monolithic PTAT temperature sensor. The measured temperature is used in a feedback loop to adjust the thermal tuner of the ring. The closed-loop feedback system is demonstrated to operate in presence of thermal perturbations at 20Gb/s.

OCIS codes: (130.4110) Modulators; (130.3120) Integrated optics devices; (230.2090) Electro-optical devices; (250.5300) Photonic integrated circuits.

References and Links

1. I. A. Young, E. Mohammed, J. T. Liao, A. M. Kern, S. Palermo, B. A. Block, M. R. Reshotko, and P. L. Chang, "Optical I/O technology for tera-scale computing," J. Solid-State Circ. **45**(1), 235–248 (2010).
2. G. Li, X. Zheng, J. Lexau, Y. Luo, H. Thacker, P. Dong, S. Liao, D. Feng, M. Asghari, J. Yao, J. Shi, P. Amberg, N. Pinckney, K. Raj, R. Ho, J. E. Cunningham, and A. V. Krishnamoorthy, "Ultralow-power, high- performance Si photonic transmitter," in *Optical Fiber Communication Conference*, 2010 OSA Technical Digest Series (Optical Society of America, 2010), paper OMI2.
3. P. Dong, S. Liao, H. Liang, W. Qian, X. Wang, R. Shafiiha, D. Feng, G. Li, X. Zheng, A. V. Krishnamoorthy, and M. Asghari, "High-speed and compact silicon modulator based on a racetrack resonator with a 1 V drive voltage," Opt. Lett. **35**(19), 3246–3248 (2010).
4. S. Manipatruni, Q. Xu, B. Schmidt, J. Shakya, and M. Lipson, "High speed carrier injection 18Gb/s silicon micro-ring electro-optic modulator," in *Proceedings of Laser and Electro-Optics Society* (2007), pp. 537–538.
5. M. R. Watts, D. C. Trotter, R. W. Young, and A. L. Lentine, "Ultralow power silicom microdisk modulators and switches," in *Proceedings of 5th IEEE International Conference on Group IV Photonics* (IEEE 2008), pp. 4–6.
6. E. Timurdogan, A. Biberman, D. C. Trotter, C. Sun, M. Moresco, V. Stojanovic, and M. R. Watts, "Automated wavelength recovery for microring resonators," in *Proceedings of Conference on Lasers and Electro-Optics* (Optical Society of America, 2012), paper CM2M.1.
7. W. Zortman, A. L. Lentine, D. C. Trotter, and M. R. Watts, "Bit-error-rate monitoring for active wavelength control of resonant modulators," IEEE Micro **33**(1), 42–52 (2013).
8. C. Qiu, J. Shu, Z. Li, X. Zhang, and Q. Xu, "Wavelength tracking with thermally controlled silicon resonators," Opt. Express **19**(6), 5143–5148 (2011).
9. J. A. Cox, A. L. Lentine, D. C. Trotter, and A. L. Starbuck, "Control of integrated micro-resonator wavelength via balanced homodyne locking," Opt. Express **22**(9), 11279–11289 (2014).
10. B. Guha, B. B. Kyotoku, and M. Lipson, "CMOS-compatible athermal silicon microring resonators," Opt. Express **18**(4), 3487–3493 (2010).
11. C. T. DeRose, M. R. Watts, D. C. Trotter, D. L. Luck, G. N. Nielson, and R. W. Young, "Silicon microring modulator with integrated heater and temperature sensor for thermal control," in *Proceedings of Conference on Lasers and Electro-Optics* (Optical Society of America, 2010), paper CThJ3.
12. Y. Zhang, T. Baehr-Jones, R. Ding, T. Pinguet, Z. Xuan, and M. Hochberg, "Silicon multi-project wafer platforms for optoelectronic system integration," in *Proceedings of IEEE Group IV Photonics Conference* (2012), pp. 63– 65.
13. J. E. Cunningham, I. Shubin, X. Zheng, T. Pinguet, A. Mekis, Y. Luo, H. Thacker, G. Li, J. Yao, K. Raj, and A. V. Krishnamoorthy, "Highly-efficient thermally-tuned resonant optical filters," Opt. Express **18**(18), 19055–19063 (2010).

1. Introduction

As bandwidth requirement for chip-to-chip links scale, signaling over electrical channels has become extremely challenging [1]. Silicon photonics has the potential to enable low-power and high-speed chip-to-chip communication. Compact, low-power and high-speed electro-optic modulators (EOM) are one of the key components in realization of chip-to-chip optical

#242378 Received 5 Jun 2015; revised 30 Jul 2015; accepted 3 Aug 2015; published 12 Aug 2015

signaling. Resonant structures such as micro-ring modulators are promising candidates due to their compact size and low power consumption. Examples of such structures reported in the past few years include carrier-depletion micro-ring modulators [2,3], carrier-injection micro-ring modulators [4], silicon micro-disk modulators [5] and polymer ring modulators [1]. As the resonance wavelength is susceptible to temperature fluctuations, resonant modulators require thermal tuning. Sophisticated techniques and circuitry have been proposed to stabilize the temperature fluctuations in ring resonator modulators [6–11]. Examples of such techniques are output optical power feedback [6], bit error-rate (BER) feedback [7], feedback through scattered light [8] and balanced homodyne detection [9]. These techniques require extra optical power on the silicon-photonic chips or complex circuitry for implementation. There have been other attempts to reduce temperature susceptibility of micro-ring resonators using negative thermo-optic materials as an overlay on micro-ring [10]. These attempts require extra fabrication steps and do not fit standard CMOS process flows. Also, any process variation causes imperfect athermalization and fluctuations in resonance frequency. As an alternative athermalization method, micro-ring modulators with integrated temperature sensor and resistive heater have been proposed to enable thermal compensation [11]. However, this effort relies on a single diode, which is prone to process variation and requires careful consideration of die temperature gradient. Temperature gradient caused by the integrated heater and ambient thermal sources can lead to inaccurate and false temperature measurements. In this paper, we propose thermal tuning through a monolithic distributed Proportional To Absolute Temperature (PTAT) sensor. Linear operation of the temperature sensor with and without operational heater is demonstrated over 125°C. Using a temperature feedback loop, the micro-ring modulator is shown to operate at 20Gb/s in presence of emulated temperature fluctuations.

2. Device design and analysis

The basic principal behind the PTAT temperature sensor is that difference between voltage drop of two forward-biased diodes, operating at different current densities, is linearly proportional to absolute temperature. Starting from a simple diode equation, diode current (I_D) vs voltage (V_D) is approximated to be

$$V_D = \frac{nKT}{q}\ln(\frac{I_D}{I_S}) \tag{1}$$

where K is the Boltzmann constant, T is the absolute temperature, q is the charge of electron, I_s is the reverse bias saturation current and n is fabrication constant typically between 1 and 2. Two forward-biased diodes with different sizes will have a voltage difference of

$$V_{D21} = V_{D2} - V_{D1} = \frac{nKT}{q}\left(\ln(\frac{I_{D2}}{I_{S2}}) - \ln(\frac{I_{D1}}{I_{S1}})\right) = \frac{nKT}{q}\ln(N\frac{I_{D2}}{I_{D1}}) \tag{2}$$

where N is the ratio of diodes (i.e. ratio of their reverse bias saturation currents). The slope of the PTAT sensor can be engineered using the ratio of reverse bias saturation currents and ratio of currents fed to each diode. In this design, the ratio of currents is 4 and $N = 5$ resulting in a factor of 20. For a given voltage sensitivity, it is desirable to maximize the slope of PTAT sensor to achieve higher accuracy in temperature readings. However, if the difference in currents becomes too large, the difference between voltage-drops across the parasitic resistances of diodes cause error. A low-pass filter can significantly reduce the effect of device noise on overall PTAT voltage noise. However, this will limit the bandwidth of the feedback loop. Therefore, in high-speed applications with a limited power budget, there will be a minimum current that can be applied to diodes to satisfy the noise requirements. This leads to a maximum diode ratio (N).

#242378 Received 5 Jun 2015; revised 30 Jul 2015; accepted 3 Aug 2015; published 12 Aug 2015

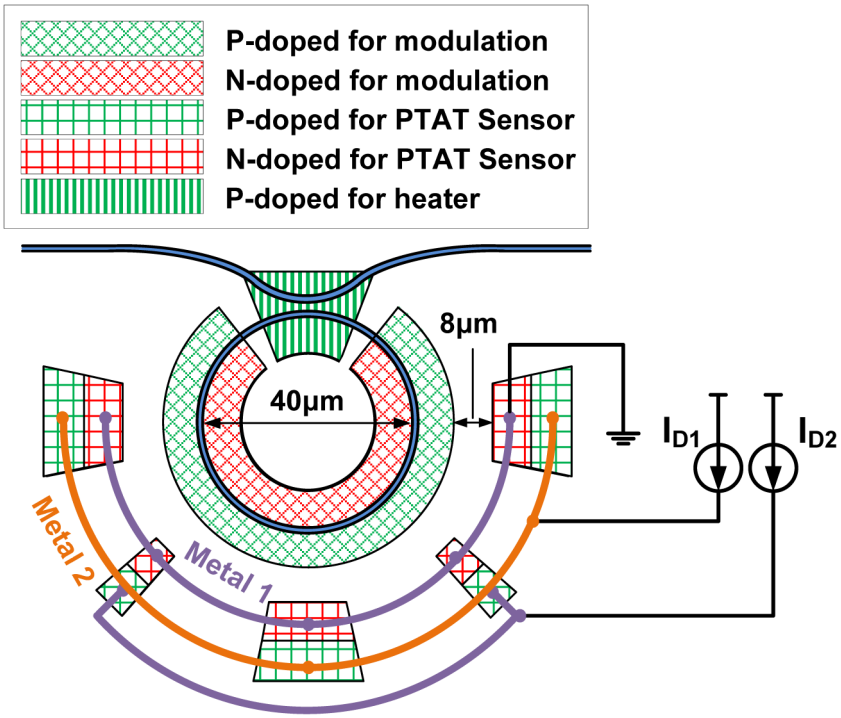

Fig. 1. Proposed structure of ring resonator with integrated heater and PTAT temperature sensor.

Designing a monolithic PTAT temperature sensor for a micro-ring modulator requires careful consideration for a number of geometric trade-offs. The temperature has to be measured accurately, which requires close proximity of PTAT temperature sensor and the ring. On the other hand, it is desirable to have the integrated heater very close to the ring and utilize maximum perimeter of the ring for modulation. Another important factor is reliability of the temperature sensor in presence of temperature gradients and operational heater. Bearing in mind all of the above, the structure of Fig. 1 is proposed. In this architecture the heater is placed under the coupler while the rest of ring's perimeter is used for modulation. The PTAT temperature sensor is formed by two distributed diodes around the ring. Different segments of each diode are connected by two metal layers. Cathodes of both diodes are connected to ground and anode of each diode is connected to a current source. The distance between the PTAT sensor and the ring has to be minimized to the extent that no leakage between the P-doped region of the modulator and N-doped region of the sensor occurs. In this design this distance is chosen to be 8μm, which ensures no leakage. The device is designed in IME platform through OpSIS, which enables interconnection of distributed PTAT temperature sensor using two metal layers [12].

#242378 Received 5 Jun 2015; revised 30 Jul 2015; accepted 3 Aug 2015; published 12 Aug 2015

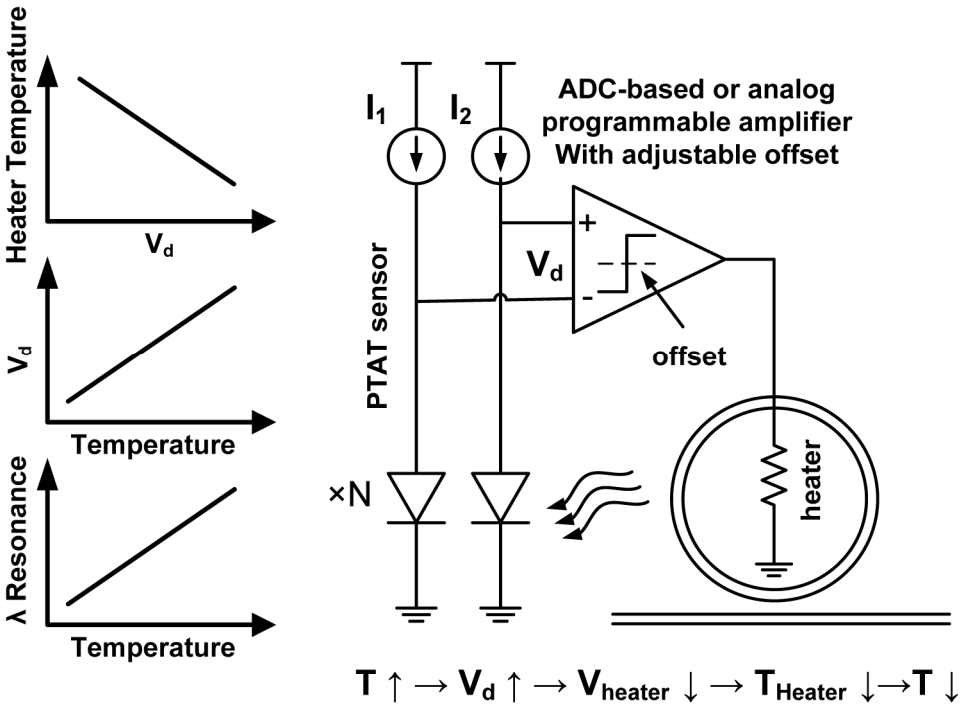

Fig. 2. Concept of a feedback loop to stabilize micro-ring's temperature.

The PTAT temperature sensor is used in a feedback loop to stabilize temperature of the micro-ring (Fig. 2). The feedback works by directly measuring the temperature of the ring and applying a heater voltage proportional to temperature error. Temperature error is defined as the difference between target temperature and ring's temperature. In a fully integrated system, the feedback loop can employ a programmable gain amplifier (PGA) or an ADC-based digital feedback to maintain a constant temperature. The target temperature is set by the offset introduced in PGA or ADC. The two current sources need to be temperature independent and stable. These current sources can be implemented using bandgap current sources. We have designed a separate CMOS chip that comprises of modulator drivers, bandgap current sources and programmable gain amplifier. In this demo, GPIB programmable SourceMeters and voltage supplies are used to test performance of the silicon photonic chip.

Figure 3 shows COMSOL heat transfer simulation of the proposed structure when the heater is off and the ring is being self-heated by the absorbed light (a) and when the heater is on (b). The distributed nature of the PTAT sensor makes it minimally susceptible to errors due to temperature gradients. From the first simulation, different fragments of the PTAT sensor see the same temperature isosurface from the first simulation. Also, when the heater is on with maximum power, more than 75% of the ring has less than 10% temperature difference with components of the PTAT sensor. Figure 4 shows the die micrograph of the micro-ring modulator with integrated heater and PTAT sensors. Total active area of the ring and PTAT sensor is less than 100μm × 100μm. Total area of the test chip including pads and grating couplers is 700μm × 200μm.

#242378 Received 5 Jun 2015; revised 30 Jul 2015; accepted 3 Aug 2015; published 12 Aug 2015

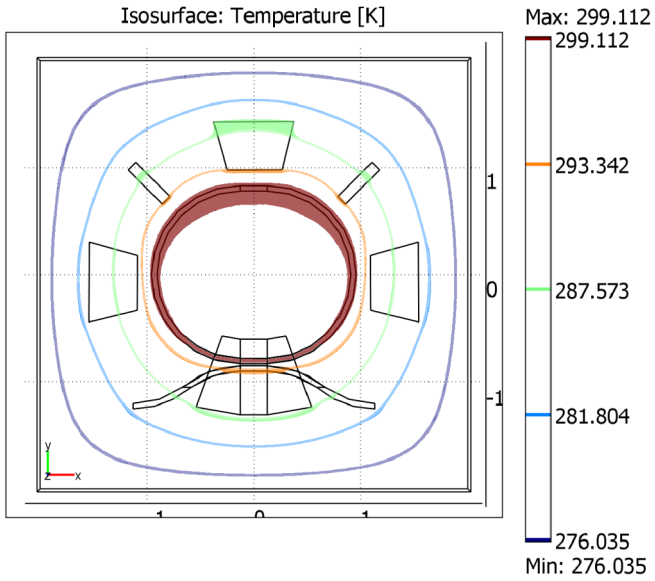

(a)

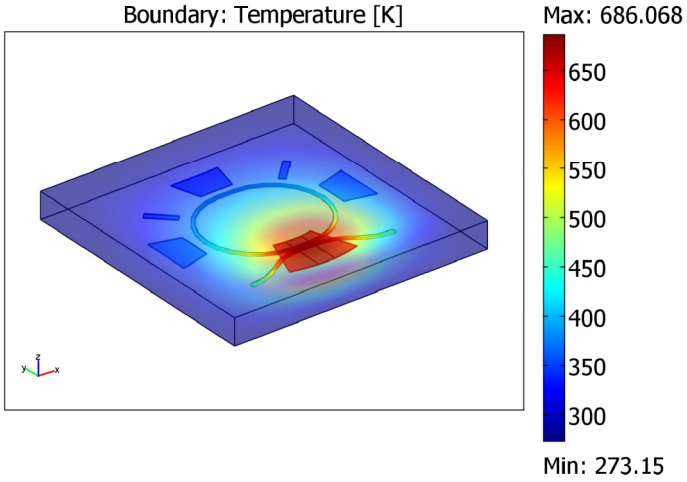

(b)

Fig. 3. COMSOL heat transfer simulations (a) Temperature uniformity across distributed PTAT sensor (b) Effect of temperature gradient due to heater on PTAT sensor.

3. Device performance characterization

The prototype was fully characterized via both DC and high-speed measurements. The DC characteristics of the micro-ring are shown in Fig. 5. The full-width half-maximum of the transmission spectra is measured to be 0.33nm resulting in a Q of around 4700 (Fig. 5(a)).

#242378 Received 5 Jun 2015; revised 30 Jul 2015; accepted 3 Aug 2015; published 12 Aug 2015

Tunability of the ring is measured to be 0.12nm/mW (Fig. 5(b)). The free spectral range (FSR) of the micro-ring is measured to be 5nm. In order to characterize the performance of the PTAT sensor, a heater is attached to the die and the difference between diode voltages versus temperature is measured. As mentioned earlier, the diodes are designed with a ratio of $N = 5$. The DC currents used for the PTAT sensor are 2.5μA and 10μA. Total power dissipated in the diodes of the sensor is approximately 9μW. Note that it is important to keep this power dissipation low to avoid heating up the PTAT's junction. The residual contact, via and wire-bond resistance is estimated to be less than 45Ω for diodes. To minimize voltage drop across this resistance, i.e. error in PTAT temperature reading, diode currents are kept low. The saturation currents are measured to be 2×10^{-18}A and 10^{-17}A for the smaller and larger diode respectively. For every wavelength the corresponding notch wavelength is also measured. Figure 5(c) illustrates these measurements and the linear equation fitted to predict the temperature from PTAT readings.

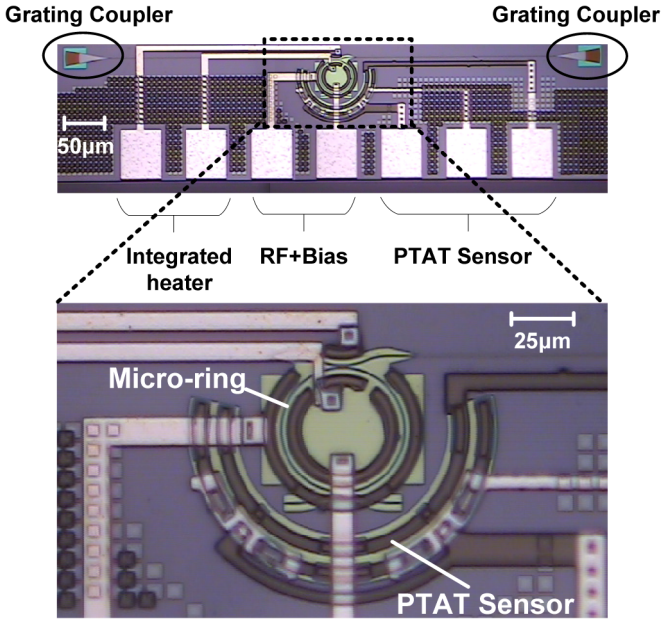

Fig. 4. Die micrograph of the fabricated micro-ring modulator with integrated heater and PTAT temperature sensor.

Functionality of the micro-ring modulator is first verified without ambient thermal noise. An RF probe is used to modulate the micro-ring and optical probes are used for carrying CW beam of laser to the input grating coupler and from output grating coupler. A high-speed PRBS-15 sequence is then used with a reverse bias of –3.5V and peak-to-peak modulation depth of 5.5V at 10Gb/s and 20Gb/s (Fig. 6). The mico-ring achieves up to 20Gb/s of data rate with an extinction ratio of 4dB.

#242378 Received 5 Jun 2015; revised 30 Jul 2015; accepted 3 Aug 2015; published 12 Aug 2015

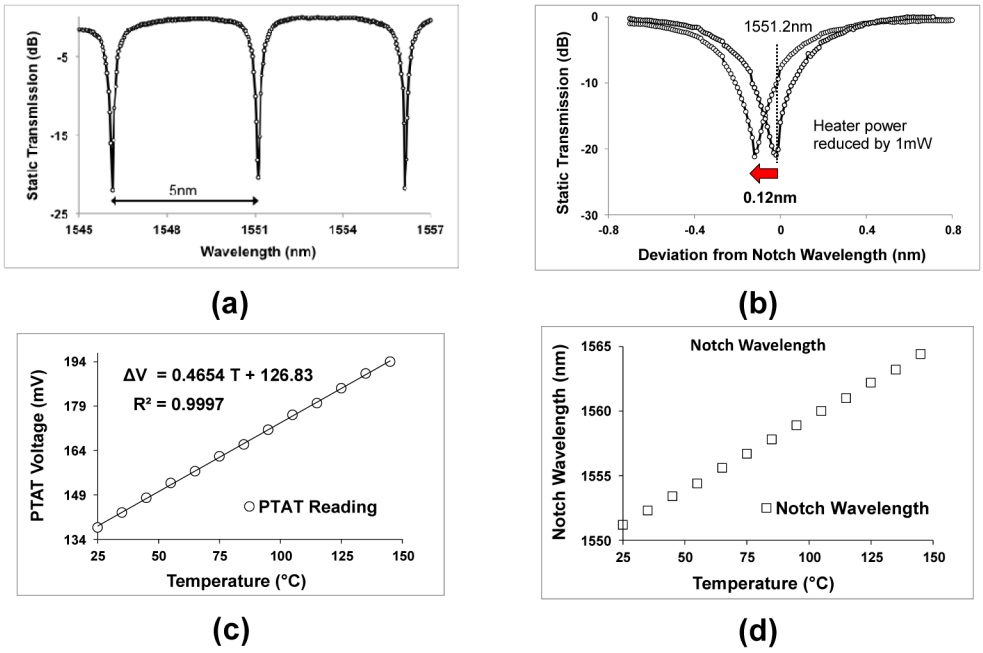

Fig. 5. (a) DC static transmission of the micro-ring (b) Measured integrated heater tunability of the micro-ring (c) Measured PTAT voltage vs temperature (d) Measured micro-ring resonance wavelength vs temperature.

Figure 7 shows the measurement setup for high-speed measurements of the modulator. A peltier thermoelectric heater/cooler is used to emulate temperature fluctuations of the ring. The peltier heater/cooler provides a maximum temperature difference of 47°C from a maximum current of 5A. The peltier cooler's current is modulated with a 0.5Hz square wave such that the temperature of the ring changes by 3.2°C every second. The feedback loop of Fig. 2 is formed using two GPIB programmable SourceMeters connected to the PTAT sensor and a programmable power supply connected to the integrated heater. The heater, which is a P-doped area under the coupling region of the micro-ring, has a resistance of 2kΩ. The SourceMeters provide constant currents of 2.5μA and 10μA for the PTAT sensor and are used to read the voltage difference between the two diodes. This voltage is then compared with a preprogramed target voltage and the difference is multiplied by −10000 and applied to the integrated heater. The pre-programed PTAT target voltage in this case was 140.3mV corresponding to 29°C. Equation (3) summarized feedback loops operation.

$$V_{Heater} = -10000 \times (V_{PTAT} - 0.1403) = -10000 \times (V_{D1} - V_{D2} - 0.1403) \qquad (3)$$

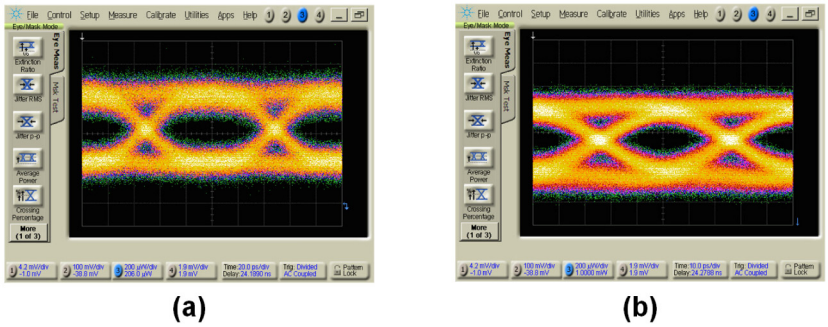

Fig. 6. High-speed optical response of the micro-ring (a) at 10Gb/s (b) at 20Gb/s.

#242378 Received 5 Jun 2015; revised 30 Jul 2015; accepted 3 Aug 2015; published 12 Aug 2015

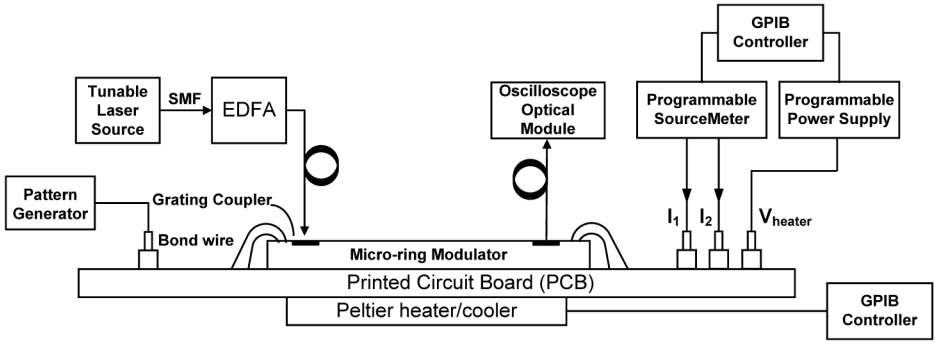

Fig. 7. High-speed measurement setup with induced thermal fluctuations and temperature stabilization feedback loop.

Without external temperature perturbations, the feedback sets the heater voltage such that micro-ring's temperature matches the target temperature of 29°C or PTAT voltage of 140.3mV. The heater voltage associated with this setting was measured to be 2.8V. Figures 8(a) and 8(b) show the peltier heater/cooler current, the PTAT voltage readings and the voltage of the integrated heater produced by the feedback loop. The heater voltage, which changes from 0.74V to 2.48V, corresponds to 2.8mW change in heater's power. According to Figs. 5(b) and 5(d), this corresponds to 3.2°C change in temperature of micro-ring. Note that due to presence of PCB, the heat slowly diffuses from peltier heater/cooler to the silicon photonic die. This is the primary limit in demonstrating higher bandwidth for the feedback loop as the PTAT sensor itself can track faster temperature fluctuations. Figure 8(c) shows the output optical eye diagram in presence of emulated ambient temperature noise without temperature stabilization feedback loop. Figure 8(d) shows the output optical eye diagram when the feedback loop is turned on.

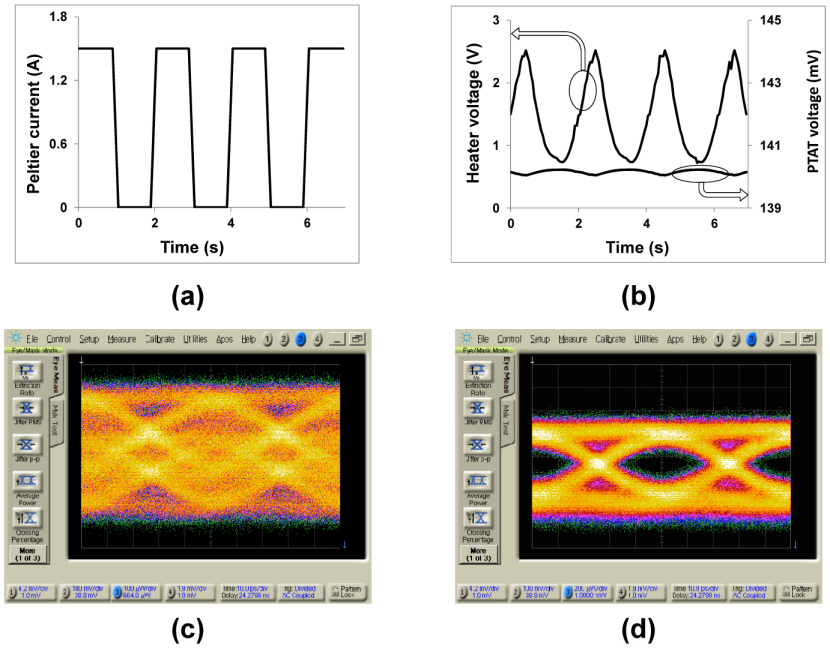

Fig. 8. (a) Peltier heater/cooler supplied current over time (b) Closed loop integrated heater voltage and PTAT voltage (c) Output optical eye diagram without thermal tuning feedback (d) output eye diagram with thermal tuning feedback.

#242378 Received 5 Jun 2015; revised 30 Jul 2015; accepted 3 Aug 2015; published 12 Aug 2015

In this experiment, the feedback loop was controlled by a GPIB programmable SourceMeters and power supplies connected to a computer; however, a low-power ADC-based feedback or programmable gain amplifier can be employed to control the heater voltage in the feedback loop. The power consumption of this temperature stabilization method, as other methods that use a heater, is dominated by the heater power. In this experiment the average heater power consumption was 1.3mW. But the heater power consumption depends on the target temperature, since it is possible to use the same heater to overcome process variation. The feedback loop can be used to set the temperature by ensuring PTAT voltage matches a pre-programed value. A one-time calibration can be used to set this value to adjust the resonance wavelength to wavelength of interest. In order to make sure we can set the resonance wavelength to any wavelength, the FSR of 5nm has to be covered. In this case 41mW is required to cover the entire FSR. This requirement can be significantly reduced by selective removal of the SOI substrate to increase thermal impedance of the device [13].

4. Conclusions

A compact micro-ring modulator with integrated heater and monolithic PTAT temperature sensor is presented. The distributed design of the PTAT sensor makes it minimally susceptible to temperature gradients. Total active area of the micro-ring including PTAT sensor (not including pads) is 100μm × 100μm. Linearity of the PTAT sensor is shown over 125°C. A temperature stabilization loop is demonstrated to compensate an ambient thermal noise. The closed-loop system operates at data-rates up to 20Gb/s in presence of temperature fluctuations.

Acknowledgments

Authors would like to thank Prof. Hajimiri and Aroutin Khachaturian for insightful discussions and OpSIS program for device fabrication.

#242378 Received 5 Jun 2015; revised 30 Jul 2015; accepted 3 Aug 2015; published 12 Aug 2015